Published in final edited form as:

J Biomed Mater Res B Appl Biomater. 2017 October ; 105(7): 1892–1905. doi:10.1002/jbm.b.33725.

Comparison of shape memory polymer foam versus bare metal coil treatments in an *in vivo* porcine sidewall aneurysm model

John Horn[1], **Wonjun Hwang**[1], **Staci L. Jessen**[1], **Brandis K. Keller**[1], **Matthew W. Miller**[2], **Egemen Tuzun**[2], **Jonathan Hartman**[3], **Fred J. Clubb Jr.**[1,4], **Duncan J. Maitland**[1]

[1]Department of Biomedical Engineering, Texas A&M University, College Station, Texas

[2]Texas A&M Institute for Preclinical Studies, Texas A&M University, College Station, Texas

[3]Department of Neurological Surgery, Kaiser Permanente Sacramento Medical Center, Sacramento, California

[4]Department of Veterinary Pathobiology, Texas A&M University, College Station, Texas

Abstract

The endovascular delivery of platinum alloy bare metal coils has been widely adapted to treat intracranial aneurysms. Despite the widespread clinical use of this technique, numerous suboptimal outcomes are possible. These may include chronic inflammation, low volume filling, coil compaction, and recanalization, all of which can lead to aneurysm recurrence, need for retreatment, and/or potential rupture. This study evaluates a treatment alternative in which polyurethane shape memory polymer (SMP) foam is used as an embolic aneurysm filler. The performance of this treatment method was compared to that of bare metal coils in a head-to-head *in vivo* study utilizing a porcine vein pouch aneurysm model. After 90 and 180 days post-treatment, gross and histological observations were used to assess aneurysm healing. At 90 days, the foam-treated aneurysms were at an advanced stage of healing compared to the coil-treated aneurysms and showed no signs of chronic inflammation. At 180 days, the foam-treated aneurysms exhibited an 89–93% reduction in cross-sectional area; whereas coiled aneurysms displayed an 18–34% area reduction. The superior healing in the foam-treated aneurysms at earlier stages suggests that SMP foam may be a viable alternative to current treatment methods.

Keywords

aneurysm; embolization; shape memory polymer; SMP foam; bare metal coils

Correspondence to: D.J. Maitland; djmaitland@tamu.edu.

Conflict of Interest Statement

Shape Memory Therapeutics, Inc. (SMT) holds the commercial license for clinical vascular embolization application of the technology described here. The authors wish to disclose that Duncan Maitland is a founder, board member, and shareholder of SMT, Jonathan Hartman is a founder, board member, shareholder and chair of the advisory board of SMT, and Wonjun Hwang is employed by and holds stock options in SMT. Fred Clubb is a shareholder in SMT.

INTRODUCTION

Intracranial aneurysms

An aneurysm is a localized bulging of a weakened arterial wall. These abnormalities may manifest as saccular structures near artery bifurcations[1,2] and are common in the intracranial vasculature where a lack of an external elastic lamina makes arteries more susceptible to aneurysm formation.[3,4] It is estimated that one in 50 adults in the United States live with one or more unruptured intracranial aneurysms. These aneurysms rupture in approximately 30,000 people per year in the United States[5] resulting in subarachnoid hemorrhage which is severely debilitating or fatal in the majority of cases.[6]

Endovascular coil treatment

Given the frequently poor outcomes following aneurysm rupture, clinical interventions are carried out to address the risk of rupture. The overall goal of aneurysm treatment is to reduce or eliminate blood flow into the aneurysm sac, thereby reducing pressures and/or shear stresses on the weakened aneurysm wall, and promoting flow stagnation and thrombosis within the aneurysm sac and subsequent healing. In recent decades, the preferred method for achieving this goal has become the endovascular transcatheter placement of bare metal coils to fill and occlude the aneurysm sac. The minimally invasive nature of these procedures is a major advantage over surgical clipping, which requires a full craniotomy to gain access to the affected artery for clip placement, with the associated risk and morbidity of open surgery. Refer to Rodriguez et al.[7] for a thorough review of many of the current and historical treatment options and their clinical outcomes.

The earliest developed and most extensively studied bare metal coils used clinically are Guglielmi Detachable Coils (GDCs).[8] These soft platinum alloy coils are pushed through a catheter that has been guided from a vascular access point, such as the femoral artery, through the vasculature to the aneurysm location. Once the catheter is placed, a coil is pushed out of the catheter into the aneurysm sac and an electrical current is applied to dissolve, via electrolysis, a link connecting the coil to the pusher, thereby releasing it into the aneurysm. The number of coils placed inside the aneurysm is dependent on the aneurysm diameter (approximately one coil per millimeter of aneurysm diameter[9]), and varies based upon the length and diameter of the coils, as well as operator preference. After placement, the coils reduce the amount of flow entering the aneurysm sac and stimulate thrombus production. Ideally, a stable clot is formed inside the aneurysm around the coils which, via the body’s healing processes, is converted to a collagen-based, scar-like structure permanently occluding the aneurysm and isolating it from the flow of the parent artery. Further, it is optimal for re-endothelialization to occur across the neck, or ostium, of the aneurysm completely excluding it from the parent artery flow and returning a normal patent shape to the lumen of the artery.

Coiling treatments quickly gained favor over clipping, accounting for approximately half of all first-choice treatment options by the year 2000,[10] largely in part because of the minimally invasive nature, quick procedural time, and lower cost; however, this technique is not without its limitations. The bioinert nature of bare metal coils elicits limited tissue response

which can lead to unorganized thrombus formation and poor aneurysm healing.[11,12] Szikora et al.[12] reported a number of coil-treated aneurysms that failed to form neointimal layers across their necks at time points as late as three years post-treatment. Further, low volume occlusions in coil-treated aneurysms can result in coil compaction over time, due to a water hammering effect from the pulsing arterial flow,[13] resulting in recanalization rates of 21–34%.[14–18] These aneurysms are susceptible to aneurysm growth, rupture or rerupture, and the growth of adjacent daughter aneurysms. In 10.3% of coil-treated aneurysms, recanalization necessitates retreatment.[19] Other issues include possible coil migration from the aneurysm sac into the parent artery,[20–22] and a risk of intraprocedural aneurysmal rupture,[23] which can have devastating consequences. Given this potential for procedural complication and suboptimal long-term healing, it is desirable to develop new technologies to enhance aneurysm treatment outcomes.

Proposed shape memory polymer foam device

As an alternative to bare metal coil treatments, the use of shape memory polymer (SMP) foams as embolic fillers has been proposed.[24–26] SMP foams are porous polymeric mate rials that are capable of actuating from a set shape to a second “memorized” shape upon an increase in bulk temperature. This allows for the foam to be compressed to a size compatible with catheter delivery and then actively actuated within an aneurysm, achieving up to a 70-fold volume expansion[27] to fill the entire intra-aneurysmal space without imposing significant stress on the aneurysm wall.[28] In addition to large volume expansions, the porous architecture of SMP foams also provide large blood-contacting surface areas (up to 1000 cm^2 per 1 cm^3 of bulk foam[29]), possess highly tortuous pathways in which blood flow is greatly reduced,[30,31] and have exhibited good biocompatibility.[24,27,32,33]

Evidence of polyurethane SMP foam’s biocompatibility and efficacy as an aneurysm treatment was reported by Rodriguez et al.[34] The authors surgically implanted SMP foam samples within constructed *in vivo* porcine vein pouch aneurysm models following the technique described by Guglielmi et al.[35] Histology after 30 and 90 days post implantation revealed progressive healing within the foam filled aneurysms marked by the presence of predominately loose to dense connective tissue within the aneurysm. After 90 days, complete formation of neointimal layers were observed across each aneurysm neck excluding the aneurysms from arterial flow. Finally, the foam elicited a reduced inflammatory response when compared to the FDA-approved sutures used to construct the aneurysm model, suggesting that the SMP foam is at least as biocompatible as clinically used biomaterials. The positive results from this study motivated the development and testing of an endovascular treatment method utilizing SMP foams.

Hwang et al.[36] proposed an aneurysm treatment method wherein a spherical implant of SMP foam is compressed and delivered through a catheter to the aneurysm site. Once the SMP foam implant is deployed into the aneurysm sac, a resistive heater core is used to raise the bulk temperature of the foam to stimulate its expansion to completely fill the aneurysm. Following expansion, the resistive heater core is retracted into the catheter and both are removed from the patient.

The goal of this study is to demonstrate the proposed method[36] under clinical conditions and to compare the proposed SMP foam aneurysm fillers to bare metal coil treatments, the current gold standard for endovascular aneurysm interventions using a head-to-head pathological comparison. The foam and bare metal coils were delivered into a porcine vein pouch model.[35] This model offers aneurysms with similar sizes to those found in the human intracranial vasculature and provides an appropriate environment for simulating human biochemistry related to thrombus formation. Thus, extrapolation of the results to the potential outcomes of utilizing these treatments clinically is possible. Device performance was assessed at 90 and 180 day time points post-implant using gross evaluation and histology to elucidate the local tissue response at intermediate stages of healing wherein the initial thrombus (timescale of minutes to days[37]) is replaced with connective tissue (timescale of weeks to months[37]).

MATERIALS AND METHODS

Bare metal coils

The bare metal coils used in the study consisted of platinum and tungsten alloy wound coils of 2D helical shape (GDCV®, Stryker Neurovascular). The GDCs had 2D helical loops of 2–8 mm diameter, and overall lengths (elongated inside the introducer) of 3–30 cm. All coils used are listed in Table I.

SMP embolization device

The SMP embolization device system consisted of an SMP foam implant and a guidewire delivery assembly with a resistive heating element for SMP foam expansion.

SMP foam synthesis and implant fabrication.—The implant was comprised of two compositions of polyurethane SMP foam (Type A & Type B) secured by friction fit. The foam types chosen represent varied ratios in the net formulation. For the Type A foam, N,N,N′,N′-Tetrakis(2-hydroxypropyl)ethylenediamine (HPED, 99%, Sigma Aldrich), 2,2′,2″-Nitrilotriethanol (TEA, 98%, Alfa Aesar), 1,6-diisocyantohexane (HDI, TCI America), and deionized (DI) water (> 17 MΩ cm purity) were used as received to synthesize the H60 SMP foams using a protocol reported previously.[27] Type A composition is based on a 60 mol % of HPED (H60) isocyanate equivalents, with the remaining mol % ratio coming from TEA. For the Type B foam, N,N,N′,N′-Tetrakis(2-hydroxypropyl) ethylenediamine (HPED, 99%, Sigma Aldrich), 2,2′,2″-Nitrilotriethanol (TEA, 98%, Alfa Aesar), 1,6-diisocyantohexane (HDI, TCI America), 1,6-diisocyantotrimethylhexane, 2,2,4- and 2,4,4- mixture (TMHDI, TCI America), and deionized (DI) water (> 17 MΩ cm purity) were used as received to synthesize the 80TM SMP foams using a protocol reported previously.[38] Type B composition is based on an 80 mol % of TMHDI (80TM) isocyanate equivalents, with the remaining mol % coming from HDI. Further, Type B incorporates a 4% by volume loading of tungsten powder (<1 μm particle size, 99.95% purity, Alpha Aesar) to facilitate visualization of the crimped implant under fluoroscopy.[33]

The two composition types were combined to create a hybrid implant with Type A core and Type B outer shell as previously reported.[36] Cylindrical samples with nominal diameters of

4.0, 6.0, and 8.0 mm, and lengths of 8–10 mm were cut from the Type A foam [Fig. 1(a)]. Utilizing computer-controlled milling (MDX-540SA, Roland DGA Corp.), spheres with diameters of 6.6, 8.8, and 11.0 mm were milled from Type B foam, with cylindrical cores of 3.0, 5.0, and 7.5 mm diameters, respectively, removed from the spheres [Fig. 1(b)]. The cylindrical samples of Type A foam were then inserted into the resulting spherical shells and trimmed to make the final hybrid SMP foam implant [Fig. 1(c)].

This hybrid device leverages the desirable properties of each foam type to achieve the treatment goals. The Type A foam core has a low density allowing for large compressions while also providing enough expansion to fill the aneurysm. While the Type B foam enables visualization during implantation, its greater density and poor expansion make it unsuitable for use as the entire implant. However, the greater hydrophobicity of Type B foam allows it to serve as a water barrier preventing the plasticization of the more hydrophilic Type A core and preventing premature expansion of the implant.

SMP foam implant processing.—To break residual foam pore membranes, the hybrid foam implants were mechanically conditioned by radially compressing and re-expanding them at 97°C using a stent crimper (SC150–42, Machine Solutions). The implants were chemically etched in a 0.1N hydrochloric acid (HCl) solution and cleaned with 20% (by volume) detergent solution (Contrad® 70, Decon Laboratories) to remove residual surfactants and catalysts from the foam fabrication process, then thoroughly rinsed with RO water to ensure all of the detergent had been removed.[38] Finally, the samples were held at 50°C under vacuum for 12 h until dry.

SMP foam implant delivery system.—The delivery system for the foam implants consisted of a hollow guidewire assembly and a resistive heating element constructed by winding nichrome wire around a nitinol core wire [Fig. 2(a)] as reported by Hwang et al.[36] The resulting resistive heaters had diameters of 0.32 ± 0.01 mm and lengths of 5.59 ± 1.14 mm [Fig. 2(b)]. The hybrid SMP foam implants were threaded onto the resistive heating element at the distal tip of the delivery system [Fig. 2(c)]. The foam was crimped over the resistive heater using a stent crimper to a final crimped diameter of 1.09 ± 0.17 mm [Fig. 2(d)] to achieve a friction fit. Each device was individually sealed in a sterilization pouch with desiccant, sterilized by ethylene oxide (EtO), and allowed to degas for 24 h before endovascular implantation.

In vivo device studies

In this study, two aneurysms were created in each animal. In all animals, one aneurysm was treated with bare metal coils and the other was treated with SMP foam. Endpoints for the study were 90 days and 180 days post-implant, both of which included two animals. While the short-term performance (30 and 90 day) of SMP foam-based devices has been previously evaluated,[34] the longer implant duration in this study allow the assessment of the devices at a more intermediate stage of healing (i.e., well after the initial clotting response and into the stages of healing wherein the initial thrombus is replaced with connective tissue).[37]

Porcine sidewall aneurysm model.—All animal experiments were conducted in accordance with policies set by the Texas A&M University Institutional Animal Care and Use Committee and met all federal requirements, as defined in the Animal Welfare Act, the Public Health Service Policy, and the Humane Care and Use of Laboratory Animals. Additionally, NIH guidelines (or for non-U.S. residents similar national regulations) for the care and use of laboratory animals (NIH Publication #85–23 Rev. 1985) were observed.

Animal studies were performed in the catheterization laboratory at the Texas A&M Institute for Preclinical Studies. Fluoroscopic visualization was achieved using a C-arm X-ray system (Allura Xper FD20, Koninklijke Philips N.V.). Saccular sidewall vein pouch aneurysm models were created in the carotid arteries of four 3 to 4 month old Yorkshire swine weighing 31.1 ± 2.8 kg using a previously described model.[35] To create the aneurysm models, the animals were placed under general anesthesia using intramuscular injection of ketamine, xylazine, and acepromazine (20 mg/kg, 2 mg/kg, and 0.2 mg/kg, respectively). The animals were intubated and anesthesia was maintained using isoflurane. Using sterile technique, access to the carotid arteries and external jugular veins was achieved by making a 10 cm incision along the ventral cervical midline and reflecting the sternocleidomastoid muscle medially. A 4 cm segment of the external jugular vein was isolated and excised, allowing for 2 cm long pouches to be created by cutting the segment transversely. After the carotid arteries were exposed and cleaned of adventitia, vascular clamps were placed to provide temporary occlusion. A 7 mm arteriotomy of the artery was created and an end-to-side anastomosis of the vein pouch to the carotid artery was performed using 7–0 polypropylene sutures. The open end of the pouch was sutured to create an 8–10 mm diameter aneurysm sac. Vein pouch aneurysms were created on the right (RCCA) and left (LCCA) common carotid arteries, resulting in two per animal [Fig. 3(a)]. Injections of contrast medium (Oxilan® 300, Guerbet) were used to visually confirm aneurysm formation under fluoroscopy [Fig. 3(b)]. After confirmation of formation, the subcutaneous tissues were loosely closed. Implant procedures were performed within 3 h of aneurysm creation.

Endovascular aneurysm access.—Treatment of the aneurysms was performed using standard endovascular technique for device delivery and implantation. A 6 Fr introducer sheath (Pinnacle®, Terumo) was inserted into the animal's femoral artery using ultrasound guidance. A 0.035 inch guidewire (Glidewire®, Terumo) was inserted and, under fluoroscopy, used to advance and place a 5–6 Fr guiding catheter (Envoy® or Neuropath®, Codman & Shurtleff) through the introducer sheath to the aneurysm site. The SMP devices were directly delivered through the guiding catheter. For delivery of GDCs, a micro catheter (Excelsior® 1018®, Stryker Neurovascular or Concourse™ 14, Micrus) was advanced and placed through the guiding catheter to the aneurysm site.

Aneurysm implant delivery and treatment.—Following catheter placement, the GDCs or crimped SMP foams were advanced through the catheter and pushed out into the aneurysm sac. GDC delivery was accomplished in the order listed in Table I. Detachment was achieved using a detachable coil power supply (M00345100840, Stryker Neurovascular). Confirmation of coil occlusion was accomplished under fluoroscopy. The SMP foam implant delivery and deployment process is shown via fluoroscopy in Figure 4.

Following the placement of the compressed foam implant within the aneurysm sac [Fig. 4(a)], the copper leads of the heating device at the proximal end of the delivery assembly were connected to a power supply (U3606A, Agilent Technologies) which delivered power outputs from resistive heating of 1.3 +/− 0.1 W for 30 sec and 0.6 +/− 0.1 W for 120 sec to provide the necessary heat stimulus to achieve foam actuation [Fig. 4(b)]. While the temperature profiles of the resistive heater were not monitored during this process, forced and free convection in combination with blood flow within the aneurysm sac provide efficient dissipation of thermal energy and prevent thermal tissue damage.[39] As the foam actuates, the friction forces holding the foam in place on the delivery device are reduced, allowing for easy removal of the heating element and device deployment [Fig. 4(c,d)]. Injections of contrast medium were used to visually confirm aneurysm occlusion and degree of contrast stagnation under fluoroscopy/angiography [Fig. 4(e,f)].

Gross evaluation and histopathology

Necropsy.—Animals were heparinized, euthanized and presented for necropsy at the preselected end time points. The vessels with devices were isolated and first rinsed with physiologic saline then perfusion fixed with 10% buffered formalin. The carotid arteries (with surrounding soft tissue) were removed *en bloc* and placed in formalin to allow for further fixation.

Neck Re-endothelialization.—After fixation, the parent vessel of each aneurysm was cut parallel to the long axis to expose the lumenal view of each aneurysm. The lumenal aspect of each aneurysm was photographed grossly with a high resolution camera (EOS-1 Mark III, Canon) to assess the degree of endothelialization of the aneurysm neck.

Histopathology.—Aneurysms with attached parent vessel and devices in situ were then processed, embedded in Technovit 7200 VLC, and sectioned and microground using a diamond saw and grinding wheel (300 CP and 400 CS, EXAKT Technologies, Inc.). Each resulting histology section was a cross-section perpendicular to the long axis [Fig. 5(a–c)]. Each aneurysm was serially sectioned in this manner to obtain slides from the entire thickness of the aneurysm. Slides were stained with Hematoxylin and Eosin (H&E) to view the cell nucleus (blue) and surrounding cytoplasm (red, pink, or orange) to evaluate general pathology including inflammation.[40]

Scoring slides/quantifying metrics.—To compare the amount and degree of inflammation versus healing response between the polymer foam and coil treatment for each time point, cell types were distinguished and counted for three different regions of each aneurysm based on well-established morphologic descriptors for each cell type.[4,40] The aneurysm was divided into three zones: central-, mid-, and outer-zone [Fig. 5(d)]. Within each zone, 300 cells were categorized as neutrophil, eosinophil, plasma cell, erythrophagocytosis, multinucleated giant cell, macrophage (with erythrocytes [erythrophagocytosis], or hemosiderin [hemisoderin-laden]), fibroblast/fibrocyte, capillary endothelial cell, or lymphocyte. Additionally, the central core was evaluated for collagen deposition, and the stage of healing was identified. The collagen concentration and overall

cell counts for each aneurysm were then assessed individually to determine the degree of inflammation/healing.

To assess the overall size of each aneurysm, the length, width, and neointima thickness of each aneurysm were measured from the microscopic slides using virtual microscope software (VS-ASW Software, Olympus Corporation) (Fig. 6). The measurements were taken from the serial section that had the greatest dimension (i.e., measurements were taken from the center most portion of the aneurysm). The length and width data were compared to the initial measurement of the aneurysms taken from fluoroscopy images on the day of the implant (Syngo Software, Siemens Corporation). The 2-D cross sectional area of each post-treatment aneurysm was estimated from the histology sections using open-source imaging software (ImageJ, National Institute of Health). Neointimal thickness was assessed by averaging five measurements across the aneurysm neck [Fig. 6(c,d)].

RESULTS

Aneurysm embolization

Angiographic imaging was performed before and after aneurysm treatment and prior to animal sacrifice at the appropriate time points (Fig. 7). Treatment with GDC coils completely occluded all aneurysms shortly after treatment [Fig. 7(a.1)]. While the SMP foam implant impeded much of the flow of contrast dye into the foam-treated aneurysms following deployment, in some cases [Fig. 7(b.1,d)], contrast dye was acutely visible. However, contrast dye injections prior to explant at 90 and 180 days [Fig. 7(c,e)] indicated complete isolation of the aneurysm from the parent artery blood flow for both treatment modalities.

In all cases, the endovascular treatments were performed without procedural complications. Established clinical expectations (i.e., adequate aneurysm occlusion without coil or foam prolapse into the parent artery) were achieved for the GDC-based and SMP foam-based aneurysm treatments. Physician feedback indicated that the SMP foam and heating device were effortlessly delivered through the guide catheter and the foams expanded within the aneurysms as expected following the application of current to the resistive heating element. In one animal (animal 3 in Table I), a second SMP foam device was implanted into the foam treated aneurysm. In this case, the first SMP foam device was not large enough to fill the aneurysm and a second, smaller device was deployed and expanded without complication.

90 day implant results

The GDC-treated aneurysms appear to have thinner walls/sacs with coils (C) bulging into the surrounding tissue spaces and lumens, whereas the SMP foam-treated aneurysms (F) are smaller and have less intrusion into surrounding areas (Fig. 8, C.90.1, F.90.1). While all aneurysms at the 90 day time point have a defined neointimal layer over the entire aneurysm ostia, the neointimal layers over the GDC-treated aneurysms are less defined, with neointima-covered coils partially protruding into the artery lumens (Fig. 8, C.90.2). Additionally, the downstream edges of the ostia of the foam-treated aneurysms show greater definition of healed neointima compared to the coil-treated aneurysms (i.e., less transparent;

Fig. 8, F.90.2). Measurements taken from the histology sections (Table II) show that the layers of re-endothelialization across the ostia of the GDC-treated aneurysms are thinner (by 19% and 37% for animals 1 and 2, respectively) and less organized (Fig. 8, C.90.3) than those formed across the ostia of the corresponding foam-treated aneurysms (Fig. 8, F.90.3). Furthermore, the neointimal layers formed across the foam-treated aneurysm ostia restore a natural curvature to the parent vessel, creating a normal vessel cross-section at the aneurysm neck (Fig. 8, F.90.3), whereas the GDCs protrude into the parent artery, yielding irregular topography (Fig. 8, C.90.3).

The length, width, and cross-sectional areas of the aneurysms at the time of implant (obtained from fluoroscopy) and at 90 days (obtained from histology) are listed in Table II. Despite their congruence at time of implantation, the foam-filled aneurysms (Fig. 8, F.90.3) show greater reduction in size than the GDC-filled aneurysms (Fig. 8, C.90.3; Table II). The SMP foam-treated aneurysms have a marked healing response as shown by the loose connective tissue in the central core with minimal, residual cellular debris and <5% immature connective tissue (Fig. 8, F.90.4). This contrasts with the coil findings where the central cores contain approximately 25–50% immature loose connective tissue and patchy residual debris (Fig. 8, C.90.4).

The 90 day histological analysis, based on the cell counts listed in Table III, also reflects a marked healing response in the SMP foam-treated aneurysms as noted by the low numbers of neutrophils, eosinophils, plasma cells, and lymphocytes (totaling <4% of cells counted per aneurysm). Similarly, all aneurysms had comparable counts of multinucleated giant cells (3–10%), endothelial cells (11–18%), and fibrocytes/fibroblasts (44–56%). However, both animals at the 90 day time point showed a noticeable difference in the number of macrophages between the coil- and the foam-treated aneurysms. There was a higher macrophage count, including those undergoing erythrophagocytosis, in the GDC-treated aneurysms than those treated with SMP foam (20–22% vs. 6–12%, respectively). The foam-treated aneurysms contained a greater count of macrophages containing hemosiderin (hemosiderin-laden macrophages) than the GDC-treated aneurysms (17–18% vs. 3–4%, respectively), primarily in the outer circumference of the aneurysm dome (113–117 vs. 3–18 cells, respectively).

180 day implant results

At 180 days post-treatment, the GDC-treated aneurysms continue to have slightly more transparent walls/sacs when compared to the SMP foam-treated aneurysms, but the differences are less prominent than between the 90 day aneurysms (Fig. 9, C.180.1, F.180.1). All aneurysms have a defined neointimal layer over each aneurysm ostium (Fig. 9, C.180.2, F.180.2). From the histology slides, it can be seen that the GDCs continue to disrupt the natural curvature of the endothelial layer at the aneurysm-parent vessel interface. The aneurysms at the 180 day time point show a larger difference in overall size (Fig. 9, C.180.3, F.180.3; Table II) than the 90 day post-treatment aneurysms. After 180 days, remaining cellular debris was observed in the GDC-treated aneurysms and approximately 50% (animal 3) and 20% (animal 4) of their central cores were comprised of loose, immature connective tissue (Fig. 9, C.180.4). One of the GDC-treated aneurysms contains multifocal areas of

calcification from regions of clotted blood and cellular debris within the core that was not completely cleared out by the macrophages. In contrast, the core of the SMP foam-treated aneurysm shows rare foci of cellular debris and mostly mature connective tissue (<5% immature connective tissue) (Fig. 9, F.180.4).

Cell counts and percentages over three regions of each aneurysm are described in Table IV. On a cellular level, the GDC- and SMP foam-treated aneurysms after 180 days showed similar trends as the 90 day time point. Cell types that tend to be involved in the acute inflammatory response (neutrophils, eosinophils, and lymphocytes) had a relatively low presence in each aneurysm (<10%), with a slightly higher presence in the coiled aneurysm of animal 4 (9.34% vs. <4% for all other aneurysms). At 180 days, the macrophage count (including those undergoing erythrophagocytosis) decreased from the 90-day time point for the coil-treated aneurysms (20–22% to 11–15%). The foam-treated macrophage count stayed relatively the same for both time points (6–12%). Additionally, the percentage of fibroblast/fibrocytes present was higher in the 180 day time point (66% vs. 56–68%) than in the 90 day time point (44–56% vs. 48–56%). The coil filled aneurysms at 180 days continue to have a lower count of hemosiderin-laden macrophages (HLMs) than the foam-filled aneurysms (0.89–4.44% vs. 10–14%). There was a decrease in the HLM count from the 90 day foam-treated aneurysms compared to the later time point, whereas the HLM count in the coil-treated aneurysms stayed below 5% for both time points.

DISCUSSION

In this research, the method of using resistive heat-actuated SMP foams[36] to endovascularly treat intracranial aneurysms was successfully demonstrated under clinical conditions in a porcine vein pouch model. Delivery of compressed SMP foam, via catheter, to the aneurysm was achieved and a resistive heating core provided adequate bulk temperature increases to stimulate foam expansion. While the delivery of the SMP foam-based devices was successful for the specific aneurysm model used in this study, it should be noted that device size (requiring 5 Fr catheter or larger for delivery) and compressed stiffness make the present design unsuitable for human intracranial applications (which require catheters smaller than 3 Fr and device flexibility to navigate the tortuous neurovasculature). Further, the low animal study size ($n = 2$ per study group) also limits the conclusions that can be drawn herein. The four animal study is not sufficient to conclude the superiority in the efficacy of the new device over the conventional treatment (platinum coils). Nonetheless, the evaluation of the SMP foams implanted in this study elucidates physiological responses to SMP foam and provides context for the anticipated local tissue healing response following human intracranial aneurysm treatment using highly porous SMP foam-based devices. The evaluation time points in this study focus on the maturation phase of the foreign body reaction. A previous study addresses earlier phases, weeks to months, where recanalization is more likely to occur.[34] In this regard, it was possible to assess the post-treatment performance of the present SMP foam implants using histological analysis and compare longer-term outcomes of foam-treated aneurysms to those treated with bare metal coils, the current standard for endovascular aneurysm intervention.

The devastating outcomes from intracranial aneurysm rupture have motivated clinical treatment with the goal of isolating the affected location from arterial blood flow. Recently, the preferred approach has become the endovascular filling of the aneurysm sac with various embolic materials and devices. The placement of bare metal coils has garnered the most use by clinicians, but this method can produce non-ideal treatment outcomes, notably poor healing resulting from suboptimal aneurysm filling that leaves the neck exposed to pulsing arterial flow that can inhibit thrombus formation and lead to immature healing at the aneurysm neck.[14–18] Attempts at resolving the filling issue have led to the development of liquid embolic materials wherein a polymer is injected in a liquid form, that is, dissolved in a solvent, and then cured or hardened to form a solid mass that completely fills the aneurysm.

In animal and human models, liquid embolic materials have been successful in isolating the aneurysm from flow and facilitating the formation of a neointimal layer across the aneurysm neck.[41,42] However, these same technologies are especially dependent on complete aneurysm filling. In cases where aneurysms were only partially filled, aneurysm rupture often occurred within 10 days following treatment.[41,42]

The present study involves a novel material that has previously shown potential as an alternative aneurysm filler, shape memory polymer foam. The bulk foam fills the entire aneurysm, and provides a roughly uniform “scaffold,” particularly in the aneurysm neck, that allows for thrombus filling, cellular infiltration, and tissue ingrowth that define a successful healing process.

In the treatment of aneurysms with bare metal coils and SMP foam embolic devices, the goal is for blood to clot immediately within the aneurysm and device, thereby reducing or eliminating blood flow into the aneurysm and effectively preventing aneurysm expansion and rupture. For current coiling techniques, the clinician assesses this initial occlusion via contrast dye injections and fluoroscopic imaging with the goal being to achieve no contrast dye visible within the treated aneurysm. The aneurysms treated in this study show patent flow of contrast within their necks [Fig. 7(B.1,D)] immediately after treatment. With coils, this differential increase in radio-opacity could indicate insufficient filling in the aneurysm neck. However, in the foams, visualization of contrast is possible with good filling as the porous foams are not radio-dense enough to block the contrast visualization. When no contrast is visible in foam-treated aneurysms, a clot is fully formed that blocks the flow. While direct evidence of the presence of foam in the aneurysm necks is not available, these same aneurysms had a fully filled sac, as evidenced by pre-explant fluoroscopic imaging [Fig. 7(C,E)], and thick fibrous cap upon explant. Also, from simulations of foam-treated aneurysm, the neck is the last location to fill with clot due to higher shear rates and less stagnation since the neck is exposed to higher blood flow velocities.[31] The lack of radio opacity in the foams is a clinical adoption challenge.

Long-term, the goal is healing of the aneurysm characterized by transition from a blood clot to a remodeled, mature collagen matrix, with a healed, re-endothelialized parent vessel across the aneurysm neck. This long-term healing begins via typical acute inflammatory response wherein neutrophils, lymphocytes and macrophages infiltrate the blood clot

(composed of fibrin and erythrocytes) present from the initial implant procedure. This acute and sub-acute inflammation then transitions to early healing (granulation tissue). At this stage, macrophages begin to remove the clot by breaking down the red blood cells (i.e., hemosiderin). Hemosiderin-laden macrophages within the soft tissue compartment migrate to the periphery in order to gain access to the circulation via lymphatic drainage. Concomitantly, macrophages and lymphocytes recruit fibroblasts to lay down a collagenous connective tissue matrix, replacing the initial fibrin clot with this extracellular matrix. Chronic inflammation is characterized by sustained macrophage and lymphocyte activity prior to the recruitment of fibroblasts,[4] and would not result in an adequately healed aneurysm filled with a mature collagen matrix. The fact that there are more hemosiderin-laden macrophages (identified as HLM in Tables III and IV) in the outer circumference than the central core of the foam-treated aneurysms indicates that these aneurysms are at an advanced stage of healing: the macrophages are in transition of leaving the site and transporting their hemosiderin-laden load to the liver for recycling. The decrease in hemosiderin-laden macrophages from 90 to 180 days in the foam-treated aneurysms further indicates advanced healing. The hemosiderin-laden macrophages have nearly completed clearing out the clot/cellular debris, and in their place, fibroblasts and mature fibrocytes are further remodeling the extracellular matrix. This is also evidenced by the increased percentage of mature connective tissue within the central core of the SMP-treated aneurysms. In contrast, the GDC-treated aneurysms are healed at rates consistent with the literature,[12,14,19] as indicated by the consistently low hemosiderin-laden macrophage count at both time points, and the presence of immature, cellular connective tissue within the central core. The low numbers of lymphocytes and plasma cells indicate that both the coil- and foam-treated aneurysms are transitioning from acute/chronic inflammation and moving toward healing.

The overall size of the foam-treated aneurysms had reduced when compared to the initial post-implant aneursym measurements (Table II) and the tissue within the foam-treated anuerysms had transitioned from granulation tissue to dense mature connective tissue. This indicates contraction of the connective tissue within the foam-treated aneurysms, which is another sign of an advanced stage of healing.

The complete re-endothelialization of the parent vessel across the ostium of each aneurysm is a key step toward healing, as this mature layer separates the aneurysm from the parent artery blood flow. The aneurysms treated with foams consistently exhibit similar remodeling and maturation at the endothelial level, with a neointima conforming to a natural, c-shaped parent artery. As with any coil-based treatment, coil protrusions into the neck of the GDC-treated aneurysms in this study resulted in a thin fibrous cap across the aneurysm neck as the coils interfered with the development of the neointimal layer.

Overall, the degree of re-endothelialization, diminution of aneurysm size, and restoration of normal appearance to the parent vessel lumen for the foam-filled aneurysms all occurred despite the low degree of initial angiographic occlusion. This encourages further investigation into the benefits for the use of porous SMP foams as embolic devices.

CONCLUSIONS

Although this study only included two aneurysms in each category (i.e., coil and foam-treatments at two time points), each set of aneurysms showed similar trends in morphological and cellular changes. Evidence for healing is most indicative within the core region of the aneurysm where inflammatory cells require infiltration to clear out cellular debris. Rapid healing of the foam-treated aneurysms is evidenced by an admixture of immature and mature collagenous connective tissue and absence of residual implant debris within the core in the early stage (90 days post-treatment), whereas the central core of the coil-treated aneurysms at this time point contained mostly immature collagenous connective tissue with residual post-implant cellular debris. However, the number of animals used in this study at each time point prevent any comparative conclusions. As a pilot study, the data reported here motivate a statistically powered comparative study between foam-containing devices and bare platinum coil-treated aneurysms. Further, as the foams used in this study were not deliverable through standard neurovascular microcatheters, a different device design is needed that includes the foams. We are presently in advanced stages of developing an appropriate foam-based device. As a whole, the gross and histological results compiled in this study suggest that SMP foams are biocompatible when used to treat aneurysms and have the potential to improve upon the short- and long-term outcomes of current aneurysm treatments. Moving forward, additional statistically powered animal studies involving early and extended time scales should be performed to support these results.

Contract grant sponsor:

National Institutes of Health/National Institute of Biomedical Imaging and Bioengineering; contract grant number: R01EB000462

REFERENCES

1. de la Monte SM, Moore GW, Monk MA, Hutchins GM. Risk factors for the development and rupture of intracranial berry aneurysms. Am J Med 1985;78(6, Part 1):957–964. [PubMed: 4014270]
2. Humphrey JD, Canham PB. Structure, mechanical properties, and mechanics of intracranial saccular aneurysms. J Elasticity Phys Sci Solids 2000;61(1–3):49–81.
3. Stehbens WE. Pathology and pathogenesis of intracranial berry aneurysms. Neurol Res 1990;12(1):29–34. [PubMed: 1970622]
4. Kumar V, Abbas AK, Fausto N, Mitchell RN, Robbins SL. Robbins Basic Pathology. Philadelphia, PA: Saunders/Elsevier; 2007 946 p.
5. Molyneux AJ, Kerr RS, Yu L-M, Clarke M, Sneade M, Yarnold JA, Sandercock P. International subarachnoid aneurysm trial (ISAT) of neurosurgical clipping versus endovascular coiling in 2143 patients with ruptured intracranial aneurysms: a randomised comparison of effects on survival, dependency, seizures, rebleeding, subgroups, and aneurysm occlusion. Lancet 2005;366(9488):809–817. [PubMed: 16139655]
6. Bederson JB, Connolly ES, Batjer HH, Dacey RG, Dion JE, Diringer MN, Duldner JE, Harbaugh RE, Patel AB, Rosenwasser RH. Guidelines for the management of aneurysmal subarachnoid hemorrhage. Stroke 2009;40(3):994–1025. [PubMed: 19164800]
7. Rodriguez JN, Hwang W, Horn J, Landsman TL, Boyle A, Wierzbicki MA, Hasan SM, Follmer D, Bryant J, Small W, Maitland DJ. Design and biocompatibility of endovascular aneurysm filling devices. J Biomed Mater Res Part A 2015;103(4):1577–1594.

8. Guglielmi G, Viñuela F, Sepetka I, Macellari V. Electrothrombosis of saccular aneurysms via endovascular approach. Part 1: Electro-chemical basis, technique, and experimental results. J Neurosurg 1991;75(1):1–7. [PubMed: 2045891]
9. Vanzin JR, Abud DG, Rezende MT, Moret J. Number of coils necessary to treat cerebral aneurysms according to each size group: a study based on a series of 952 embolized aneurysms. Arquivos de Neuro-Psiquiatria 2012;70(7):520–523. [PubMed: 22836458]
10. Raftopoulos C, Mathurin P, Boscherini D, Billa RF, van Boven M, Hantson P. Prospective analysis of aneurysm treatment in a series of 103 consecutive patients when endovascular embolization is considered the first option. J Neurosurg 2000;93(2):175–182.
11. Murayama Y, Viñuela F, Tateshima S, Song JK, Gonzalez NR, Wallace MP. Bioabsorbable polymeric material coils for embolization of intracranial aneurysms: a preliminary experimental study. J Neurosurg 2001;94(3):454–463. [PubMed: 11235951]
12. Szikora I, Seifert P, Hanzely Z, Kulcsar Z, Berentei Z, Marosfoi M, Czirjak S, Vajda J, Nyary I. Histopathologic evaluation of aneurysms treated with Guglielmi detachable coils or Matrix detachable microcoils. Am J Neuroradiol 2006;27(2):283–288. [PubMed: 16484393]
13. Kwan ES, Heilman CB, Shucart WA, Klucznik RP. Enlargement of basilar artery aneurysms following balloon occlusion—"water-hammer effect". J Neurosurg 1991;75(6):963–968. [PubMed: 1941126]
14. Raymond J, Guilbert F, Weill A, Georganos SA, Juravsky L, Lambert A, Lamoureux J, Chagnon M, Roy D. Long-term angiographic recurrences after selective endovascular treatment of aneurysms with detachable coils. Stroke 2003;34(6):1398–1403. [PubMed: 12775880]
15. Sluzewski M, van Rooij WJ, Slob MJ, Bescós JO, Slump CH, Wijnalda D. Relation between aneurysm volume, packing, and compaction in 145 cerebral aneurysms treated with coils. Radiology 2004;231(3):653–658. [PubMed: 15118115]
16. Slob MJ, van Rooij WJ, Sluzewski M. Influence of coil thickness on packing, re-opening and retreatment of intracranial aneurysms: a comparative study between two types of coils. Neurol Res 2005;27(Supplement-1):116–119.
17. Wakhloo AK, Gounis MJ, Sandhu JS, Akkawi N, Schenck AE, LinfanteI. Complex-shaped platinum coils for brain aneurysms: higher packing density, improved biomechanical stability, and midterm angiographic outcome. Am J Neuroradiol 2007;28(7):1395–1400. [PubMed: 17698550]
18. Geyik S, Ertugrul O, Yavuz K, Geyik P, Saatci I, Cekirge HS. Comparison of bioactive coils and bare platinum coils for treatment of intracranial aneurysms: a matched-pair analysis. J Neurosurg 2010;112(4):709–713. [PubMed: 19799497]
19. Ferns SP, Sprengers ME, van Rooij WJ, Rinkel GJ, van Rijn JC, Bipat S, Sluzewski M, Majoie CB. Coiling of intracranial aneurysms: a systematic review on initial occlusion and reopening and retreatment rates. Stroke 2009;40(8):e523–e529. [PubMed: 19520984]
20. Phatouros CC, McConachie NS, Jaspan T. Post-procedure migration of Guglielmi detachable coils and Mechanical detachable spirals. Neuroradiology 1999;41(5):324–327. [PubMed: 10379587]
21. Wang C, Xie X. Treatment of an unraveled intracerebral coil. Catheter Cardiovasc Intervent 2010;76(5):746–750.
22. Banerjee AD, Guimaraens L, Cuellar H. Asymptomatic delayed coil migration from an intracranial aneurysm: a case report. Case Rep Vasc Med 2011;2011:1–2.
23. Doerfler A, Wanke I, Egelhof T, Dietrich U, Asgari S, Stolke D, Forsting M. Aneurysmal rupture during embolization with Guglielmi detachable coils: causes, management, and outcome. Am J Neuroradiol 2001;22(10):1825–1832. [PubMed: 11733309]
24. Metcalfe A, Desfaits A-C, Salazkin I, Yahia LH, Sokolowski WM, Raymond J. Cold hibernated elastic memory foams for endovascular interventions. Biomaterials 2003;24(3):491–497. [PubMed: 12423604]
25. Hampikian JM, Heaton BC, Tong FC, Zhang Z, Wong CP. Mechanical and radiographic properties of a shape memory polymer composite for intracranial aneurysm coils. Mater Sci Eng C 2006; 26(8):1373–1379.
26. Maitland DJ, Small IV W, Ortega JM, Buckley PR, Rodriguez J, Hartman J, Wilson TS. Prototype laser-activated shape memory polymer foam device for embolic treatment of aneurysms. J Biomed Opt 2007;12(3):030504. [PubMed: 17614707]

27. Singhal P, Rodriguez JN, Small W, Eagleston S, Van de Water J, Maitland DJ, Wilson TS. Ultra low density and highly crosslinked biocompatible shape memory polyurethane foams. J Polym Sci Part B: Polym Phys 2012;50(10):724–737.
28. Hwang W, Volk BL, Akberali F, Singhal P, Criscione JC, Maitland DJ. Estimation of aneurysm wall stresses created by treatment with a shape memory polymer foam device. Biomech Model Mechanobiol 2012;11(5):715–729. [PubMed: 21901546]
29. Hearon K, Singhal P, Horn J, Small W, Olsovsky C, Maitland KC, Wilson TS, Maitland DJ. Porous shape-memory polymers. Polymer Reviews 2013;53(1):41–75. [PubMed: 23646038]
30. Small W, Gjersing E, Herberg JL, Wilson TS, Maitland DJ. Magnetic resonance flow velocity and temperature mapping of a shape memory polymer foam device. BioMed Eng OnLine 2009;8:42. [PubMed: 20043833]
31. Ortega JM, Hartman J, Rodriguez JN, Maitland DJ. Virtual treatment of basilar aneurysms using shape memory polymer foam. Ann Biomed Eng 2013;41(4):725–743. [PubMed: 23329002]
32. Cabanlit M, Maitland D, Wilson T, Simon S, Wun T, Gershwin ME, Van de Water J. Polyurethane shape-memory polymers demonstrate functional biocompatibility in vitro. Macromol Biosci 2007;7(1):48–55. [PubMed: 17238230]
33. Rodriguez JN, Yu Y-J, Miller MW, Wilson TS, Hartman J, Clubb FJ, Gentry B, Maitland DJ. Opacification of shape memory polymer foam designed for treatment of intracranial aneurysms. Ann Biomed Eng 2012;40(4):883–897. [PubMed: 22101759]
34. Rodriguez JN, Clubb FJ, Wilson TS, Miller MW, Fossum TW, Hartman J, Tuzun E, Singhal P, Maitland DJ. *In vivo* response to an implanted shape memory polyurethane foam in a porcine aneurysm model. J Biomed Mater Res Part A 2014;102(5):1231–1242.
35. Guglielmi G, Ji C, Massoud TF, Kurata A, Lownie SP, Viñuela F, Robert J. Experimental saccular aneurysms. Neuroradiology 1994; 36(7):547–550. [PubMed: 7845580]
36. Hwang W, Singhal P, Miller MW, Maitland DJ. In vitro study of transcatheter delivery of a shape memory polymer foam embolic device for treating cerebral aneurysms. J Med Dev 2013;7(2): 020932.
37. Anderson JM. Biological responses to materials. Annu Rev Mater Res 2011;31(1):81–110.
38. Singhal P, Boyle A, Brooks ML, Infanger S, Letts S, Small W, Maitland DJ, Wilson TS. Controlling the actuation rate of low-density shape-memory polymer foams in water. Macromol Chem Phys 2013;214(11):1204–1214. [PubMed: 25530688]
39. Maitland DJ, Metzger MF, Schumann D, Lee A, Wilson TS. Photo-thermal properties of shape memory polymer micro-actuators for treating stoke. Lasers Surg Med 2002;30(1):1–11. [PubMed: 11857597]
40. Brown GG. Primer of Histopathologic Technique. New York: Appleton-Century-Crofts; 1969.
41. Becker TA, Preul MC, Bichard WD, Kipke DR, McDougall CG. Preliminary investigation of calcium alginate gel as a biocompatible material for endovascular aneurysm embolization *in vivo*. Neuro-surgery 2007;60(6):1119–1128.
42. Brennecka CR, Preul MC, Bichard WD, Vernon BL. *In vivo* experimental aneurysm embolization in a swine model with a liquid-to-solid gelling polymer system: initial biocompatibility and delivery strategy analysis. World Neurosurg 2012;78(5):469–480. [PubMed: 22120570]

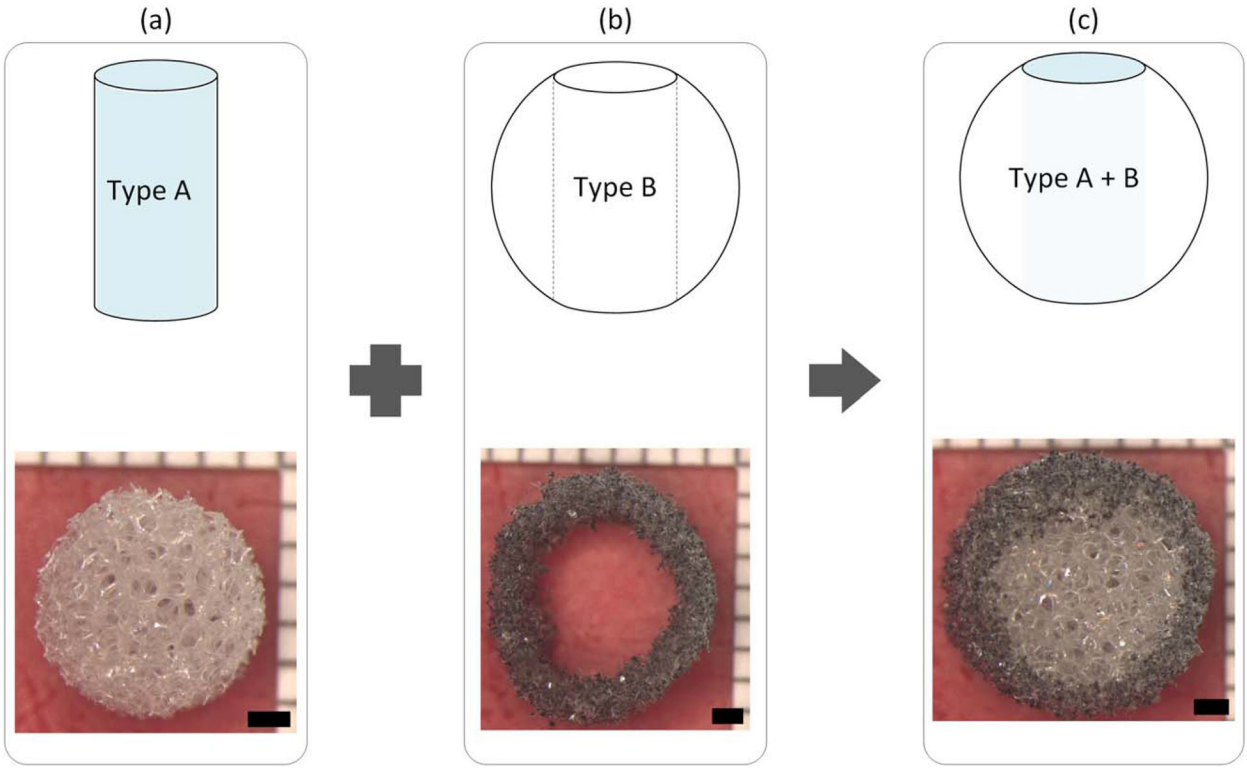

FIGURE 1.

The SMP foam implant is comprised of an inner Type A (H60) composition core (a) and a Type B (tungsten-loaded 80TM) composition outer shell (b), resulting in the final hybrid SMP foam implant (c). The upper images depict a side view schematic of the process; the lower images display top view examples of the actual implant and assembly, respectively. Scale bars −1 mm.

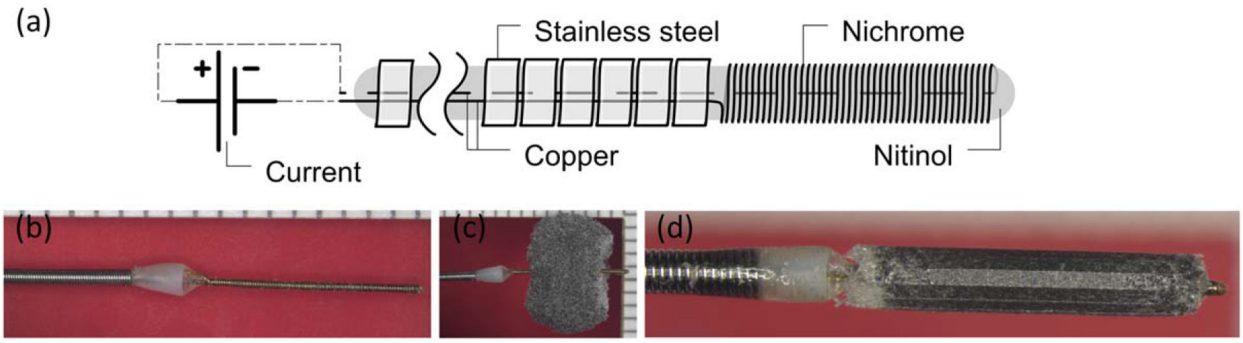

FIGURE 2.

Fabrication process of SMP embolic device. (a) Schematic and (b) photo of delivery system with resistive coil at distal end; (c) The SMP foam threaded over the resistive heating element; (d) The foam radially compressed using a clinical stent compression device. Image in panel (a) reproduced from Hwang et al.[36] with permission from ASME.

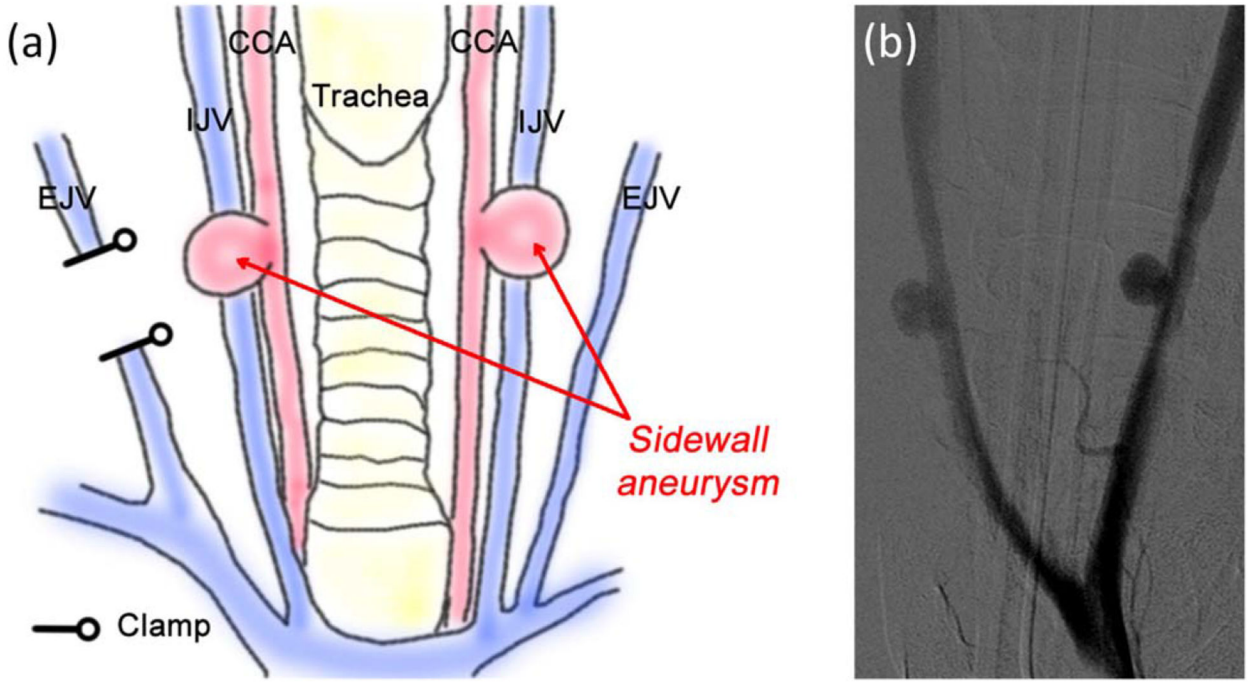

FIGURE 3.

(a) Schematic of the vein pouch aneurysm model construction. Aneurysm created on the right and left common carotid arteries (CCA) by transversally segmenting the external jugular vein (EJV); (b) Confirmation of aneurysm construction via fluoroscopic angiography. IJV-Internal jugular vein.

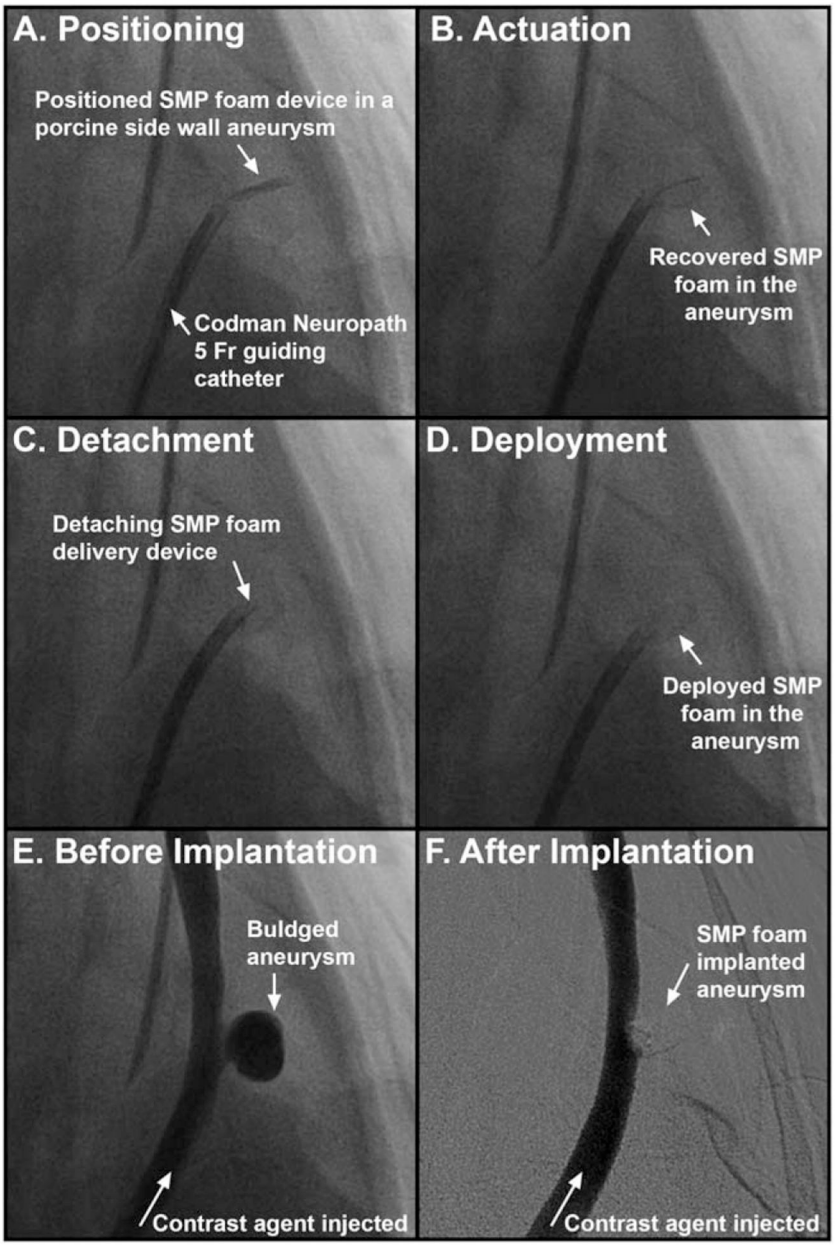

FIGURE 4.

Fluoroscopic imaging of the SMP foam treatment process. The SMP foam is positioned via guide catheter in the aneurysm sac (a). As the SMP foam recovers or actuates to its expanded shape (b), the foam friction decreases allowing detachment from the delivery device (c) and release in to the aneurysm (d). Contrast dye injections are used to visualize the aneurysm before (e) and after (f) treatment with SMP foam.

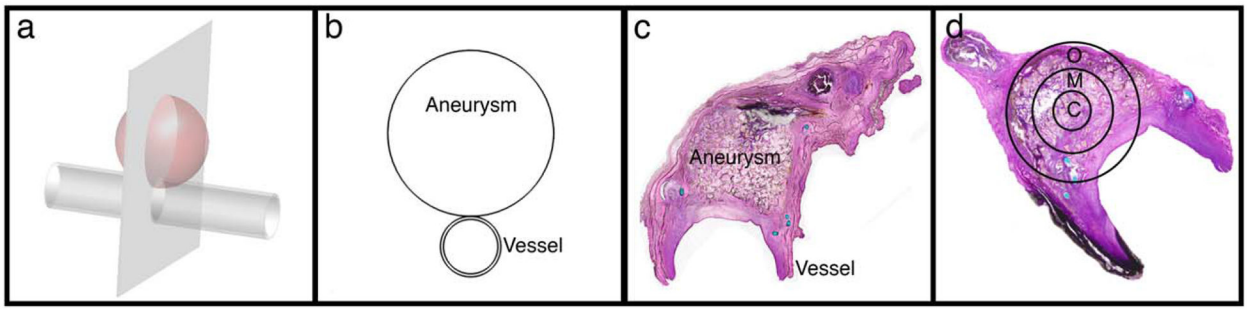

FIGURE 5.

Histology sectioning and evaluation. (a) Schematic of vessel with aneurysm showing plane of histology sections; (b) Resulting cross-section of aneurysm and vessel for histology slides; (c) Example histology section; (d) Definition of zones used for evaluating each histology section: C – Central, M – Mid, O – Outer.

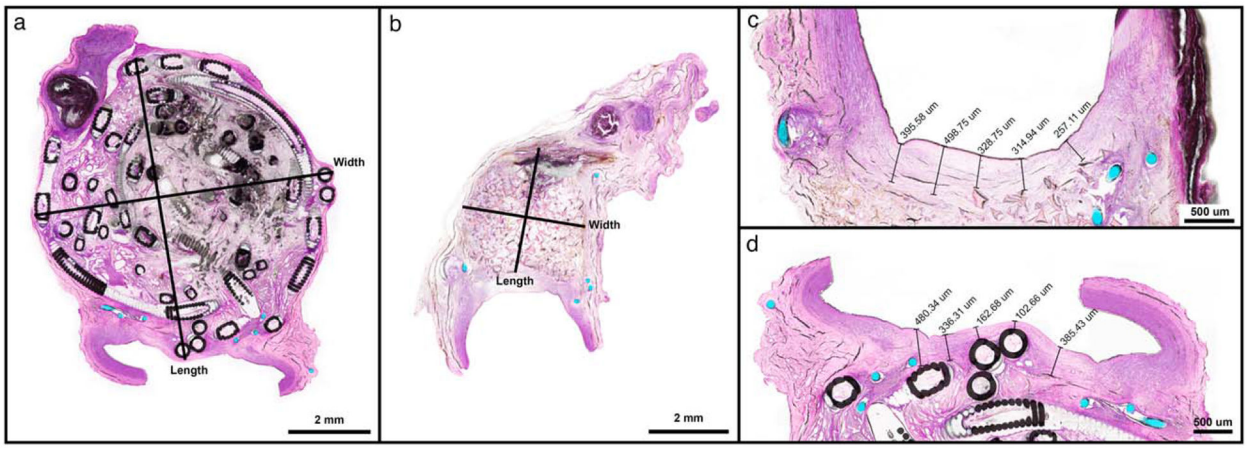

FIGURE 6.

Examples of length and width measurements for (a) GDC-filled aneurysm and (b) foam-filled aneurysm. Magnified aneurysm ostia of foam-filled (c) and GDC-filled (d) specimens for acquiring average ostium thickness.

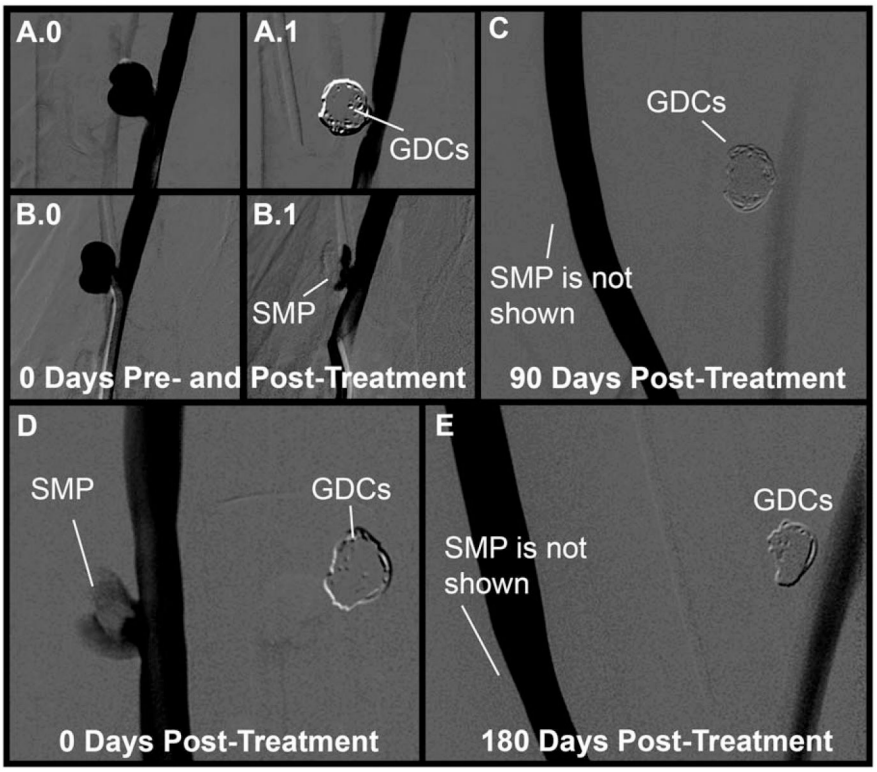

FIGURE 7.

Fluoroscopic imaging of aneurysms with contrast dye injections pre- and post-treatment, and pre-explant at 90 and 180 days. The top row shows the 90 day aneurysms before treatment with coils (a.0) and SMP foam (b.0), immediately after treatment (a.1) and (b.1), respectively, and prior to explant after 90 days (c). The bottom row shows the 180 day aneurysms immediately after treatment with SMP foam (d) and prior to explant after 180 days (e).

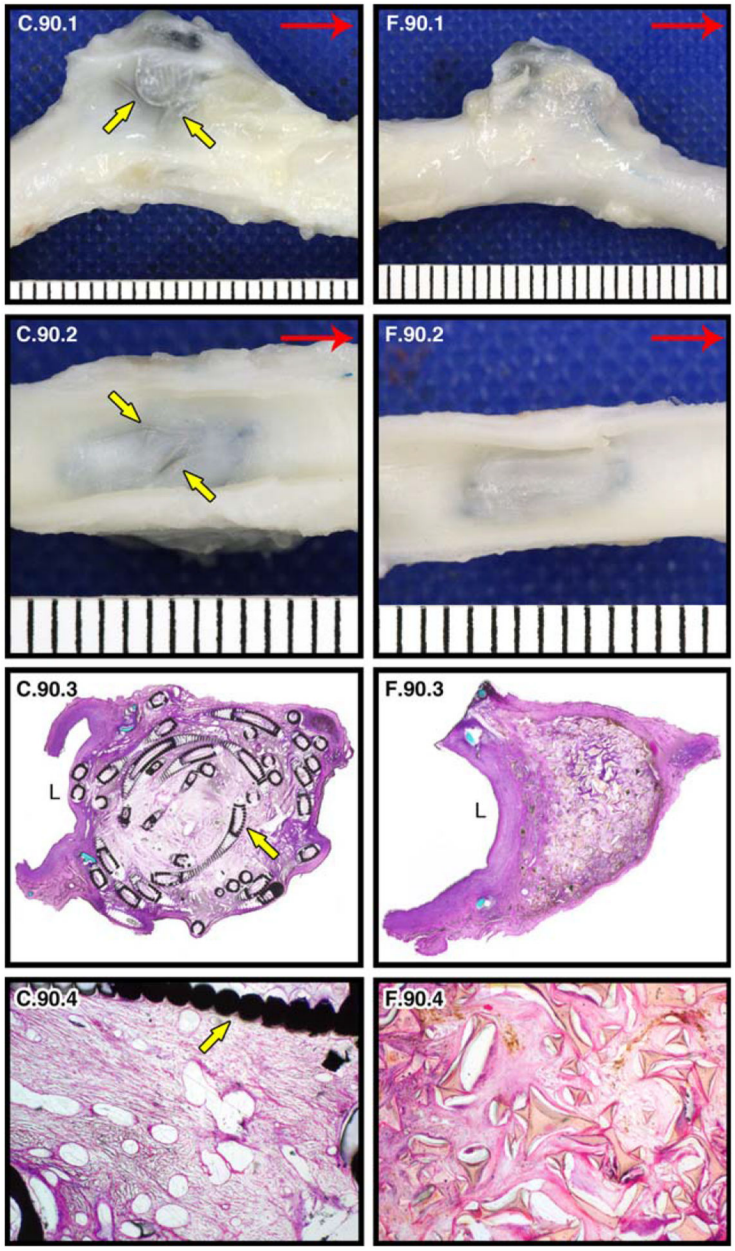

FIGURE 8.

90 day pathology of GDC-treated (c) and SMP foam-treated (f) porcine carotid artery sidewall aneurysms. Yellow arrows indicate coils. Gross images of left and right carotids at 90 days post implantation (red arrow indicates blood flow direction): lateral view of GDC-treated left carotid aneurysm (C.90.1); lateral view of SMP foam-treated right carotid aneurysm (F.90.1); *En face* lumenal views of aneurysms showing ostium of aneurysm sac (C.90.2, F.90.2). Histological evaluation of aneurysms bisected perpendicular to the long axis ("L" indicates the parent artery lumen): 2× H&E stained (C.90.3, F.90.3) and 10× H&E stained (central core; C.90.4, F.90.4) histology slides.

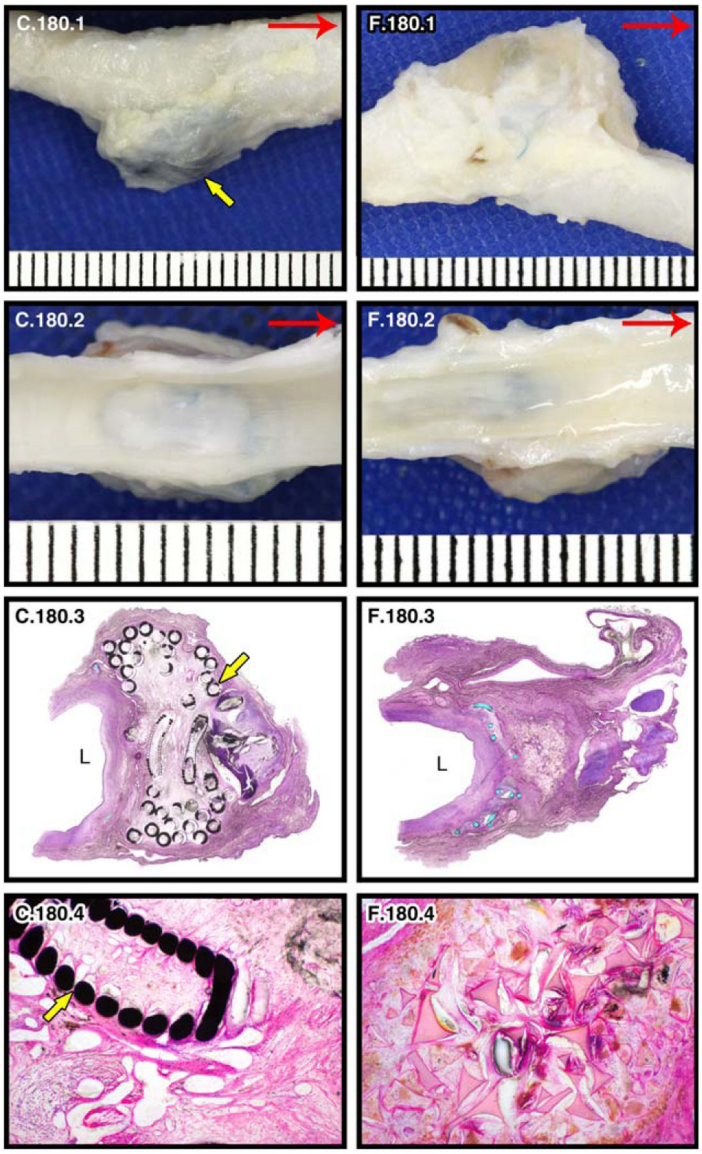

FIGURE 9.

180 day pathology of GDC-treated (c) and SMP foam-treated (f) porcine carotid artery sidewall aneurysms. Yellow arrows indicate coils. Gross images of left and right carotids (red arrow indicates blood flow direction): lateral view of GDC-treated left carotid aneurysm (C.180.1); lateral view of SMP foam-treated right carotid aneurysm (F.180.1); *En face* lumenal views of aneurysms showing ostium of aneurysm sac (C.180.2, F.180.2). Histological evaluation of aneurysms bisected perpendicular to the long axis ("L" indicates the parent artery lumen): 2× H&E stained (C.180.3, F.180.3) and 10× H&E stained (central core; C.180.4, F.180.4) histology slides.

TABLE I.

Device Implant Samples Used in the *In vivo* Study

Animal ID (Follow-Up Days)	Aneurysm Location*	Implant Material	# Implants Per Aneurysm Sac	Implant IDs by Implant Order**
Animal 1 (90 days)	LCCA	Coil	6	GDC 18 2D 8X30, GDC 10 2D 5X15, GDC 18 Soft
	RCCA	Foam	1	SMP 8X6.3
Animal 2 (90 days)	LCCA	Foam	1	SMP 7.4X6.3
	RCCA	Coil	8	GDC 18 2D 6X20, GDC 18 2D 6X20, GDC 10 2D 5X15, GDC 10 2D 5X15, GDC 10 Soft 3X6, GDC 10 Soft 3X6, GDC 10 Soft 2X3, and GDC 10 Soft 2X3
Animal 3 (180 days)	LCCA	Coil	3	GDC 18 2D 6X20, GDC 18 Soft 4X10, and GDC 18 Soft 2X4
	RCCA	Foam	2	SMP 6.4X5.4 and SMP 5.8X5.3
Animal 4 (179 days)	LCCA	Coil	4	GDC 18 2D 8X30, GDC 10 2D 5X15, GDC 18 2D 6X20, GDC 10 Soft 3X6, GDC 10 Soft 2X3, and GDC 10 Soft 2X3
	RCCA	Foam	1	SMP 8.8X6.6

*LCCA – Left common carotid artery; RCCA – Right common carotid artery.

**example, GDC 18 2D 8X30 indicates 0.0135–0.015 inch wound coil diameter, 2D helical shape, 8 mm loop diameter and 30 cm length; GDC 10 Soft 3X6 indicates 0.010 inch wound coil diameter, 2D helical shape, 3 mm loop diameter and 6 mm length; SMP 8X6.3 means 8 mm diameter outer shell and 6.3 mm height cylindrical sample for the SMP hybrid foam implant.

TABLE II.

Measurements of Intra-Aneurysmal Dimensions

		Implant (Fluoroscopy)			90 day (Histology)				Avg. Neointima Thickness (mm)
		Length (mm)	Width (mm)	Area (mm^2)	Length (mm)	Width (mm)	Area (mm^2)	% Decrease	
Animal 1	Coil	8.8	9.3	61.5	7.43	7.30	37.13	39.62%	0.29
Animal 2	Coil	6.5	7.8	41.8	6.81	5.80	26.75	36.04%	0.27
Animal 1	Foam	6.1	8.4	39.2	2.55	3.22	6.89	82.42%	0.36
Animal 2	Foam	6.1	8.5	51.1	2.82	2.99	7.22	85.59%	0.43
		Implant (Fluoroscopy)			180 Day (Histology)				Avg. Neointima Thickness (mm)
		Length (mm)	Width (mm)	Area (mm^2)	Length (mm)	Width (mm)	Area (mm^2)	% Decrease	
Animal 3	Coil	5.7	6.6	32.9	4.07	6.18	20.09	38.88%	0.67
Animal 4	Coil	7.1	8.8	51.7	7.96	7.01	42.57	17.63%	0.56
Animal 3	Foam	6.6	8.1	38.5	1.54	2.47	2.59	93.26%	0.62
Animal 4	Foam	6.6	8.4	56.3	3.24	1.75	6.2	88.98%	0.40

J Biomed Mater Res B Appl Biomater. Author manuscript; available in PMC 2020 July 24.

TABLE III.

Cell Types Within Each Aneurysm (90 Day)

	Animal 1								Animal 2								
	Foam				Coil				Foam				Coil				
	Central	Mid	Outer	Total*	Central	Mid	Outer	Total*	Central	Mid	Outer	Total*	Central	Mid	Outer	Total*	
Neutrophil	7	3	1	1.22%	3	5	3	1.22%	0	1	3	0.44%	2	0	0	0.22%	Neutrophil
Eosinophil	0	0	0	0.00%	2	0	0	0.22%	0	0	0	0.00%	0	0	0	0.00%	Eosinophil
Lymphocyte	4	5	3	1.33%	0	7	11	2.00%	1	8	9	2.00%	7	8	8	2.56%	Lymphocyte
Macrophage	37	43	23	11.44%	63	57	50	18.89%	13	31	10	6.00%	68	64	51	20.33%	Macrophage
Erythrophag.	0	0	0	0.00%	11	8	4	2.56%	1	0	1	0.22%	0	0	0	0.00%	Erythrophag.
HLM	20	29	113	18.00%	7	7	18	3.56%	23	13	117	17.00%	24	4	3	3.44%	HLM
MNGC	31	24	4	6.56%	31	30	28	9.89%	29	18	15	6.89%	7	7	12	2.89%	MNGC
EC	49	35	34	13.11%	60	53	41	17.11%	35	36	32	11.44%	51	42	37	14.44%	EC
F/F	152	161	122	48.33%	123	133	145	44.56%	198	193	113	56.00%	141	175	189	56.11%	F/F
Plasma Cell	0	0	0	0.00%	0	0	0	0.00%	0	0	0	0.00%	0	0	0	0.00%	Plasma Cell

Erythophag. – Erythrophagocytosis; HLM – Hemosiderin Laden Macrophage; MNGC – Multinucleated Giant Cell; EC – Endothelial Cell; F/F – Fibroblast/Fibrocyte.

*Total: percentage of cell type per whole aneurysm.

TABLE IV.

Cell Types Within Each Aneurysm

(180 Day)

	Animal 3								Animal 4								
	Foam				Coil				Foam				Coil				
	Central	Mid	Outer	Total*	Central	Mid	Outer	Total	Central	Mid	Outer	Total	Central	Mid	Outer	Total	
Neutrophil	0	1	1	0.22%	2	0	0	0.22%	0	3	0	0.33%	1	3	4	0.89%	Neutrophil
Eosinophil	0	0	0	0.00%	0	1	3	0.44%	0	0	0	0.00%	7	20	25	5.78%	Eosinophil
Lymphocyte	3	6	7	1.78%	10	9	6	2.78%	2	5	6	1.44%	10	9	5	2.67%	Lymphocyte
Macrophage	23	26	14	7.00%	34	47	21	11.33%	37	29	41	11.89%	46	30	53	14.33%	Macrophage
Erythrophag.	0	0	0	0.00%	2	1	0	0.33%	0	0	0	0.00%	0	0	0	0.00%	Erythrophag.
HLM	2	9	81	10.22%	4	4	32	4.44%	7	64	53	13.78%	3	2	3	0.89%	HLM
MNGC	11	16	16	4.78%	6	6	11	2.56%	6	6	3	1.67%	3	14	20	4.11%	MNGC
EC	31	26	17	8.22%	50	29	28	11.89%	36	47	51	14.89%	23	11	12	5.11%	EC
F/F	230	216	164	67.78%	192	203	199	66.00%	212	146	146	56.00%	207	211	176	66.00%	F/F
Plasma Cell	0	0	0	0.00%	0	0	0	0.00%	0	0	0	0.00%	0	0	2	0.22%	Plasma Cell

Erythophag. – Erythrophagocytosis; HLM – Hemosiderin Laden Macrophage; MNGC – Multinucleated Giant Cell; EC – Endothelial Cell; F/F – Fibroblast/Fibrocyte.

*Total: percentage of cell type per whole aneurysm.